

1,5-二硒杂[5]二茂铁环蕃的铜(I)配合物的合成、 晶体结构和电化学性质研究

景 苏^{*,1,2} 李志文¹ 顾诚云¹

(¹ 南京工业大学理学院, 南京 210009)

(² 南京大学配位化学国家重点实验室, 南京 210093)

摘要: 合成了 1,5-二硒杂[5]二茂铁环蕃的铜(I)配合物,并用 X-射线衍射单晶结构分析确定了其结构。配体的较小环径导致与铜离子配位时必须改变构型。电化学研究表明,由于 2 个二茂铁基团 Fe...Fe 的化学键距离为 1.269(2)~1.277(3) nm,因此存在强电化学联系。

关键词: 1,5-二硒杂[5]二茂铁环蕃; 铜; 晶体结构; 电化学

中图分类号: O614.121; O614.81+1; O613.52

文献标识码: A

文章编号: 1001-4861(2009)07-1212-05

Copper(I) Complex of 1,5-Diselena[5]ferrocenophane: Synthetic, Crystallographic and Electrochemical Study

JING Su^{*,1,2} LI Zhi-Wen¹ GU Cheng-Yun¹

(¹ School of Science, Nanjing University of Technology, Nanjing 210009)

(² State Key Laboratory of Coordination Chemistry, Nanjing University, Nanjing 210093)

Abstract: The copper(I) complex of 1,5-diselena [5]ferrocenophane (L) has been synthesized and the X-ray crystal structure is reported. The small cavity of the macrocyclic ligand means that the ring must undergo a conformational change to allow coordination. Electrochemical studies showed that electronic communication between ferrocenylene groups was observed in the copper complex where the through-bond Fe...Fe distances are in the range of 1.269(2)~1.277(3) nm. CCDC: 699681.

Key words: 1,5-diselena[5]ferrocenophane; copper; crystal structure; electrochemistry

0 Introduction

The design of macrocyclic systems which are capable of detecting, amplifying or recognizing metal ions has attracted more and more efforts^[1]. In this context, [n]ferrocenophanes ($n > 3$) are of great interest because of the unique chemical properties resulting from the functionality of the side arm. Some oxa- and aza-ferrocenophanes have been reported to be good

sensors for s-block cations^[2~5]. Sulphur analogues haven't been extensively studied, a few analogues with soft S-donors show good affinity to soft metal cations^[6~9].

Up to now, there are only two synthetic reports of polyselena [n]ferrocenophanes ($n > 3$), 1,4-diselena [4]ferrocenophane, 1,5-diselena [5]ferrocenophane^[10] and 1,4,7-triselena [7]ferrocenophane^[11]. As softer donor ligands, selenoferrocenophanes are expected to have a

收稿日期: 2009-03-03。收修改稿日期: 2009-04-28。

江苏省高校自然科学基金(No.08kjb150008),教育部留学回国人员启动基金。

*通讯联系人。E-mail: sjing@njut.edu.cn

第一作者: 景 苏, 女, 39 岁, 副教授; 研究方向: 配位化学和电化学分子识别。

rich chemistry, and may work as highly sensitive electrochemical sensors for the late transition metal cations. A series of acyclic ferrocenylchalcogenide ligands have been reported and studied the electronic influence of ferrocenyl substituents in soft ligand systems and metal complexes^[12-14]. We now extend the study to 1,5-diselena [5]polyselenaferrocenophane. In this paper, the synthesis, characterization, and electrochemistry of copper complex of 1,5-diselena[5]ferrocenophane (L) are described.

1 Experimental

1.1 Materials and general procedures

All the reactions were carried out under nitrogen using standard Schlenk techniques. All solvents used in the reactions were distilled over elemental alkali metal or Na/K alloy except ethanol (which was degassed before use) and dichloromethane (which was distilled over calcium hydride). 1,2,3-Triselena [3]ferrocenophane, $\text{FcSe}_3(\text{Fc}=[\text{Fe}(\eta^5\text{-C}_5\text{H}_4)(\eta^5\text{-C}_5\text{H}_4)])$, was prepared following the previously reported method^[15].

1.2 Physical measurements

^1H and ^{13}C NMR spectra were recorded on a Bruker AV500 spectrometer at 500.1 MHz and 125.8 Hz respectively, with tetramethylsilane as internal standard. Chemical shifts (δ) are reported in ppm; J values are given in Hz. NMR spectra were recorded in CDCl_3 solutions. Mass spectra were recorded using positive ion electrospray (ES); m/z values have been rounded to the nearest integer or half-integer. Assignments are based on isotopomers containing ^1H , ^{12}C , ^{16}O , ^{56}Fe , ^{80}Se , and ^{63}Cu ; expected isotope distribution patterns were observed. Cyclic Voltammetry (CV) was performed at room temperature in a dry acetonitrile solution containing $0.1 \text{ mol} \cdot \text{L}^{-1}$ $[\text{NBu}_4]\text{PF}_6$ electrolyte using an Autolab PGSTAT30 potentiostat system. The sweep rate was $100 \text{ mV} \cdot \text{s}^{-1}$ (CV). A three-electrode arrangement was used with a Pt working electrode, a Pt wire counter electrode and a Ag/Ag^+ ($0.01 \text{ mol} \cdot \text{L}^{-1}$ AgNO_3 in MeCN) reference electrode.

1.3 Synthesis

L: FcSe_3 (0.422 g, 1 mmol) was dissolved in EtOH (100 mL); NaBH_4 (0.300 g, 8 mmol) was then added.

After stirring for 2 h, the mixture became homogeneous. An ethanol solution of $\text{Br}(\text{CH}_2)_3\text{Br}$ (1 mL, 4% V/V, 1 mmol) was added, and the mixture left to stir for 4 h at room temperature. The solvent was removed by evaporation under reduced pressure. The residue was treated with water (25 mL) and extracted with CH_2Cl_2 ($3 \times 25 \text{ mL}$). The extract was dried over MgSO_4 , evaporated to dryness, then subjected to column chromatography on SiO_2 . The target product, an orange solid (0.312 g, 80%), was obtained by elution with hexane/dichloromethane (1:1). ^1H NMR (CDCl_3): 4.38 (C_5H_4 , H_{2+5} , s, 4H), 4.23 (C_5H_4 , H_{3+4} , s, 4H), 3.46 (SeCH_2 , m, 4H), 2.13 ($\text{CH}_2\text{CH}_2\text{CH}_2$, m, 2H). ^{13}C NMR (CDCl_3): 79.2 (C_1), 72.2 (C_5H_4 , C_{2+5}), 68.3 (C_5H_4 , C_{3+4}), 33.3 ($\text{CH}_2\text{CH}_2\text{CH}_2$), 25.2 (SeCH_2 , $^1J_{\text{Se-C}}=51 \text{ Hz}$). ES MS: 386 ($[\text{M}]^+$).

$[\text{CuL}_2]\text{PF}_6$: A solution of $[\text{Cu}(\text{NCMe})_4]\text{PF}_6$ (0.056 g, 0.15 mmol) in MeCN was added into a solution of L (0.116 g, 0.3 mmol) in THF. The reaction mixture was refluxed for 30 min and then allowed to cool to room temperature. After the addition of diethyl ether, the solution was kept overnight in a refrigerator. The resulting yellow crystals were collected by filtration. Yield 0.079 g (63%). ES MS: 835 ($[\text{M-PF}_6]^+$), 449 ($[\text{M-PF}_6\text{L}]^+$).

1.4 Single crystal structure determination

The crystals of the Cu(I) complex suitable for X-ray diffraction was obtained by slow evaporation from a mixed MeCN- CH_2Cl_2 - CH_3OH solution of $[\text{CuL}_2]\text{PF}_6$. The crystal with dimensions of $0.20 \text{ nm} \times 0.19 \text{ nm} \times 0.18 \text{ nm}$ was selected for structure analysis. X-ray diffraction data was collected at room temperature on a Bruker Smart Apex CCD diffractometer using graphite-monochromatized $\text{Mo K}\alpha$ radiation ($\lambda=0.071\,073 \text{ nm}$). Intensity data sets were corrected for absorption by a multi-scan procedure with SADABS^[16] and the structures was determined by direct methods, with SHELXTL^[16]. All non-hydrogen atoms were refined anisotropically using full-matrix least-squares procedures based on F^2 values and hydrogens were placed in idealized positions, each riding on the respective carrier atom. Crystal data and structure parameters are summarised in Table 1. Selected bond angles and distances are listed in Table 2.

CCDC: 699681.

Table 1 Crystal data and structure refinement for $[\text{CuL}_2]\text{PF}_6 \cdot 0.5\text{CH}_3\text{OH}$

Empirical formula	$\text{C}_{26.5}\text{H}_{30}\text{CuF}_6\text{Fe}_2\text{O}_{0.5}\text{PSe}_4$	Calculated density / ($\text{Mg} \cdot \text{m}^{-3}$)	2.024
Formula weight	992.55	Absorption coefficient / mm^{-1}	6.099
T / K	293(2)	$F(000)$	958
Wavelength / nm	0.071 073	Crystal size / mm	0.20×0.19×0.18
Crystal system	Triclinic	θ range for data collection / ($^\circ$)	1.80~26.00
Space group	$P\bar{1}$	Limiting indices	$-14 \leq h \leq 13, -10 \leq k \leq 15, -14 \leq l \leq 15$
a / nm	1.154 75(9)	Reflections collected	8 798
b / nm	1.216 3(1)	Independent reflections (R_{int})	6 236 (0.018 0)
c / nm	1.252 5(1)	Observed reflections [$I > 2\sigma(I)$]	5 072
$\alpha / (^\circ)$	105.232(1)	Data / restraints / parameters	6 236 / 1/ 379
$\beta / (^\circ)$	95.811(1)	Goodness-of-fit on F^2	1.114
$\gamma / (^\circ)$	103.152(1)	Final R indices R_1, wR_2 [$I > 2\sigma(I)$]	0.0584, 0.1584
Volume / nm^3	1.628 3(2)	R indices R_1, wR_2 (all data)	0.0474, 0.1510
Z	2	Largest diff. peak and hole / ($\text{e} \cdot \text{nm}^{-3}$)	1 276, -707

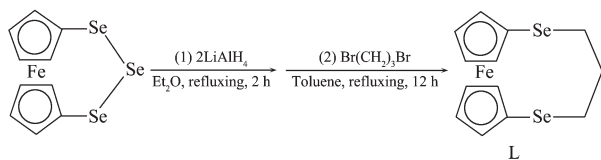
Table 2 Selected bond lengths (nm) and bond angles ($^\circ$) for $[\text{CuL}_2]\text{PF}_6 \cdot 0.5\text{CH}_3\text{OH}$

M1-Se1	0.240 0(1)	M1-Se2	0.242 4(1)	M1-Se3	0.240 7(1)
M1-Se4	0.244 8(1)	Fe1-C5	0.203 1(5)	Fe1-C9	0.204 5(5)
Fe2-C18	0.203 3(6)	Fe2-C22	0.204 0(6)	Se1-C5	0.191 2(6)
Se1-C6	0.193 7(8)	Se2-C9	0.190 9(5)	Se2-C8	0.196 5(8)
Se3-C18	0.190 2(5)	Se3-C19	0.196 0(8)	Se4-C22	0.190 8(6)
Se4-C21	0.198 2(8)				
Se1-M1-Se2	102.28(3)	Se1-M1-Se3	118.21(4)	Se1-M1-Se4	106.40(4)
Se2-M1-Se3	116.39(4)	Se2-M1-Se4	112.45(3)	Se3-M1-Se4	101.04(3)

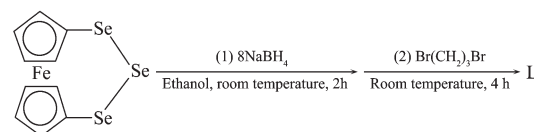
2 Results and discussion

2.1 Synthesis of L and the Cu(I) complex

The ligand 1,5-diselena[5]ferrocenophane (L) has been previously reported by the route outlined in Scheme 1^[10], this scheme is time consuming (14 h) with low yield (54.8%). We now develop a mild and efficient route with high yield, the target ligand was obtained by the sequence shown in Scheme 2. After isolated by column chromatography on silica gel using dichloromethane/hexane as eluant, the product was obtained as an orange solid in high yield (80%), which suggests that the ferrocene has the correct geometry for ring closure via a [1+1] cyclisation process.



Scheme 1



Scheme 2

Multinuclear NMR study of L shows that the ^1H and ^{13}C NMR resonances undergo a low field shift compared to those of the open chain compound $\text{FcSe}(\text{CH}_2)_3\text{SeFc}$, especially the ipso-carbon atoms bound to selenium which are at 79.3 ppm compared to 69.2 ppm in $\text{FcSe}(\text{CH}_2)_3\text{SeFc}$. The same chemical shift was observed for the ipso-carbon atoms in 1,1'-bis(methylseleno)ferrocene^[17]. In the ^1H NMR spectrum the protons of the Cp rings appeared as two well separated broad singlets at $\delta=4.38$ and 4.23 ppm (4:4), which suggest a nearly parallel conformation of the two rings in solution.

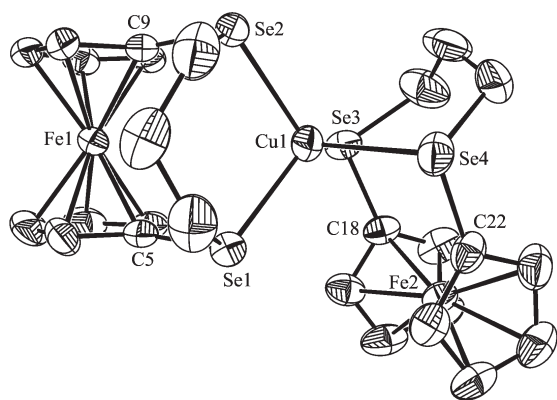
The complex $[\text{CuL}_2]\text{PF}_6$ was obtained by reaction of $[\text{Cu}(\text{NCMe})_4]\text{PF}_6$ with 2 molar equivalents of L. The electrospray mass spectra showed molecular ion peaks

with the correct isotopic pattern. The NMR spectrum of the complex shows broad features with little shifted from free ligand which may due to slow pyramidal inversion at room temperature^[12,18].

2.2 Crystal structure

The copper compound crystallized as a methanol solvate of general formula $[\text{CuL}_2]\text{PF}_6 \cdot 0.5\text{CH}_3\text{OH}$ in the triclinic space group $P\bar{1}$. There are two crystallographically independent molecules in a unit cell.

As the cavity of the L ring is quite small, it's assumed that the cation will change the conformation of the macrocycle to allow the complexation. The structure of $[\text{CuL}_2]^{2+}$ (Fig.1) shows a discrete mononuclear cation comprising two bidentate ferrocenophane ligands coordinated to a Cu(I) center giving a distorted tetrahedral coordination geometry. The angles formed by the two Se atoms attached to the same 1,1'-ferrocenylene group are compressed, $101.04(3)^\circ$ and $102.28(3)^\circ$ for Se-Cu-Se, which means the Se-M-Se angles involved in the six-membered rings are restricted by the small chelate bite of the ligand. The Cu-Se distances are within the range of $0.240\,0(1)\sim 0.244\,8(1)$ nm, and these compare well with those reported for selenoether complexes^[19,20].



Thermal ellipsoids are drawn at the 50% probability level
Hydrogen atoms are omitted for clarity

Fig.1 View of the cation in the structure of $[\text{CuL}_2]^{2+}$

The structure of the copper complex shows no significant lengthening of the ferrocenyl (sp^2) C-Se bond distances after complexation, which is quite different from the case in $[\text{M}\{\text{FcSe}(\text{CH}_2)_3\text{SeFc}\}_2](\text{PF}_6)_2 \cdot 2\text{MeCN}$ ($\text{M}=\text{Pd}$ or Pt)^[12]. This could be due to the difference between d^8 and electron rich d^{10} metal centres. The

intramolecular Se...Se distance becomes smaller on complexation: $0.298\,3$, $0.375\,6$ nm. The intramolecular Cu...Fe distance is $0.406\,5$ or $0.402\,7$ nm.

2.3 Electrochemistry

Cyclic voltammetry (CV) was used to investigate the electrochemistry of the complexes in dry acetonitrile solution. All the $E_{1/2}$ values listed below are with respect to $\text{FcH}/[\text{FcH}]^+$. In the case of $E_{1/2}$ the separation of E_a and E_c is given in brackets. The CVs of L, $[\text{CuL}_2]\text{PF}_6$ are shown on the same scale in Fig.2.

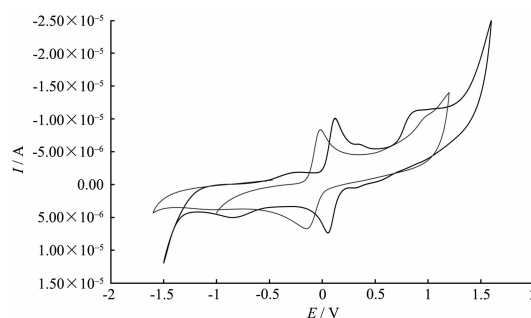


Fig.2 Cyclic voltammogram of L (—), $[\text{CuL}_2]\text{PF}_6$ (---) in dry acetonitrile, $0.1\text{ mol}\cdot\text{L}^{-1}$ tetrabutylammonium hexafluorophosphate at a scan rate of $100\text{ mV}\cdot\text{s}^{-1}$

1,2,3-Triseleno[3]ferrocenophane has an unusually high oxidation potential (213 mV)^[21], which is believed to be due to the ring strain and the interaction between the middle selenium atom in the bridge and the iron. We recorded the cyclic voltammogram of FcSe_3 for comparison purposes, and measured $E_{1/2}=232(67)\text{ mV}$. The cyclic voltammogram (CV) of L showed one clearly reversible one-electron oxidation process, with $E_{1/2}$ value of $2(115)\text{ mV}$.

In previous electrochemistry studies of $\text{FcE}(\text{CH}_2)_n\text{EFc}$ ^[22], $[\text{M}\{\text{FcE}(\text{CH}_2)_3\text{E}'\text{Fc}\}_2](\text{PF}_6)_2$ ($\text{M}=\text{Pd}$ or Pt ; $\text{E}, \text{E}'=\text{Se}$ or Te)^[12] and $[\text{M}'(\text{CO})_4\{\text{FcE}(\text{CH}_2)_3\text{E}'\text{Fc}\}]$ ($\text{M}=\text{Cr}, \text{Mo}$ or W)^[13], it was noted that the through-bond $\text{Fe}\cdots\text{Fe}$ distance must be less than a certain minimum value (in the range of $1.317\sim 1.337$ nm) for interaction between the ferrocene moieties to be observed.

The cyclic voltammogram of $[\text{CuL}_2]\text{PF}_6$ shows two closely spaced quasi-reversible steps, each with a i_a/i_c ratio of unity in the scan range $50\text{ mV}\cdot\text{s}^{-1}$ to $300\text{ mV}\cdot\text{s}^{-1}$. The cyclic voltammogram showed $E_{1/2}(1)=28\text{ mV}$ and $E_{1/2}(2)=270\text{ mV}$. If these two steps corresponding to the redox processes at the iron centres of the ferrocenes,

calculated from the crystal structure, the through-bond Fe \cdots Fe distances are in the range of 1.268 5(24)~1.277 4(25) nm, which is short enough for strong communication to occur. The difference between the two potentials (ΔE) is 242 mV. Complexes [M{FcSe(CH₂)₃SeFc}]₂(PF₆)₂ (M=Pd or Pt) have similar through bond Fe \cdots Fe distances (M=Pd, 1.275 nm; M=Pt, 1.271 nm) with similar ΔE (M=Pd, ΔE =201 mV; M=Pt, ΔE =246 mV)^[12]. But closer inspection of the CV reveals their peak current intensities are extremely different, the first one is about double of the second. Literature work has shown that the redox reaction of the Cu(I)L/Cu(II)L is chemically reversible in the copper complexes of selenium coronands. Also the π -acidity of the selenoether will result in the stabilization of Cu(I) ion and the anodic shift of the redox potential Cu(I)/Cu(II)^[23]. So we tentatively attribute the first wave to the unresolved two redox processes, Cu(I)/Cu(II) and Fe(II)/Fe(III).

The lowest oxidation potential of the complex is a little more positive than that of the “free” ligand L. As Cu(I) do not have the electron-withdrawing nature of the M(II) (M=Pd, Pt) centre, this effect can be assigned to the weak through-space interaction Cu \cdots Fe. As the macrocyclic ring is too small for the metal to reside within the cavity, the Cu \cdots Fe distance is too long for complexation to have a large effect on the half-wave potential of the 1,1'-ferrocenylene group.

References:

- [1] Constable E C. *Coordination Chemistry of Macrocyclic Compounds*. New York: Oxford University Press Inc., **1999**.
- [2] Saji T. *Chem. Lett.*, **1986**,**3**:275~276
- [3] Caballero A, Lloveras V, Tàrraga A, et al. *Angew. Chem. Int. Ed.*, **2005**,**44**:1977~1981
- [4] Tàrraga A, Espinosa A, Velasco M D, et al. *Dalton Trans.*, **2006**:3685~3692
- [5] Otón F, Espinosa A, Tàrraga A, et al. *Chem. Eur. J.*, **2007**,**13**:5742~5752
- [6] Sato M, Watanabe H, Ebine S, et al. *Chem. Lett.*, **1982**:1753~1756
- [7] Sato M, Tanaka S, Ebine S, et al. *Bull. Chem. Soc. Jpn.*, **1984**,**57**:1929~1934
- [8] Sato M, Anano H. *J. Organomet. Chem.*, **1998**,**555**:167~175
- [9] Sato M, Tanaka S, Ebine S, et al. *J. Organomet. Chem.*, **1985**,**282**:247~253
- [10] Li P, Shi S J. *Chem. J. Chin. Univ.*, **1992**,**13**:770~773
- [11] Akabori S, Takunohoshi Y, Takagi S. *Synth. Commun.*, **1990**,**20**:3187~3191
- [12] Jing S, Morley C P, Webster C A, et al. *Dalton Trans.*, **2006**:4335~4342
- [13] Jing S, Morley C P, Webster C A, et al. *J. Organomet. Chem.*, **2008**,**693**:2310~2316
- [14] Jing S, Morley C P, Webster C A, et al. *Eur. J. Inorg. Chem.*, **2008**,**32**:5067~5075
- [15] Black A J, Gould R O, Osborne A G. *J. Organomet. Chem.*, **1986**,**308**:297~302
- [16] Bruker 2000, *SMART (Version 5.0)*, *SAINT-plus (Version 6)*, *SHELXTL (Version 6.1)*, and *SADABS (Version 2.03)*, Bruker AXS Inc., Madison, WI, USA, **2000**.
- [17] Honeychuck R V, Okoroafor M O, Shen L H, et al. *Organometallics*, **1986**,**5**:482~490
- [18] Levason W, Orchard S D, Reid G, et al. *J. Chem. Soc., Dalton Trans.*, **1999**:2071~2076
- [19] Black J R, Champness N R, Levason W, et al. *Inorg. Chem.*, **1996**,**35**:4432~4438
- [20] Batchelor R J, Einstein F W B, Gay I D, et al. *J. Organomet. Chem.*, **1991**,**411**:147~157
- [21] Ushijima H, Akiyama T, Kajitani M, et al. *Chem. Lett.*, **1987**:2197~2200
- [22] Burgess M R, Jing S, Morley C P. *J. Organomet. Chem.*, **2006**,**691**:3484~3489
- [23] Batchelor R J, Einstein F E B, Gay I D, et al. *Inorg. Chem.*, **2000**,**39**:2558~2571